

Self-assembled monolayers formed by $[\text{M}(\text{CN})_5(\text{pyS})]^{4-}$ ($\text{M} = \text{Fe}, \text{Ru}$) on gold: a comparative study on stability and efficiency to assess the cyt c heterogeneous electron transfer reaction

Izaura Cirino Nogueira Diógenes,^a Jackson Rodrigues de Sousa,^a
Idalina Maria Moreira de Carvalho,^a Márcia Laudelina Arruda Temperini,^b
Auro Atsushi Tanaka^c and Ícaro de Sousa Moreira^{*a}

^a Departamento de Química Orgânica e Inorgânica, Universidade Federal do Ceará,
Caixa Postal 12200, Campus do Pici, 60455-760 Fortaleza (CE), Brazil.

E-mail: icarosm@dqi.ufc.br

^b Instituto de Química da Universidade de São Paulo-USP, Cidade Universitária,
Caixa Postal 26077, 05599-970 São Paulo (SP), Brazil

^c Departamento de Química, Universidade Federal do Maranhão, 65080-040 São Luís – (MA),
Brazil

Received 22nd November 2002, Accepted 27th March 2003

First published as an Advance Article on the web 23rd April 2003

A comparative study involving SAMs formed by $[(\text{CN})_5\text{M}(\text{pyS})]^{4-}$ inorganic complexes ($\text{M} = \text{Fe}, \text{Ru}$; $\text{pyS} = 4$ -mercaptopyridine) on gold (MpySAu) has been performed. The characterization data for these complexes suggests that the ruthenium complex exhibit a greater π -back-bonding effect that more strongly stabilizes the MpyC–S bond, thus anticipating its application as a SAM that would better enhance the gold adlayer stability than the iron complex. The MpySAu electrodes were characterized by SERS and electrochemical (LSV) techniques. The *ex situ* SERS spectra data for both SAMs suggest a σ interaction between the gold and sulfur atom of the complexes, inducing a perpendicular arrangement in relation to the surface. The spectra performed for freshly prepared MpySAu adlayers did not show any significant changes that would reflect the degradation of the adlayer. The LSV desorption curves of the SAMs indicate a better enhancement in the C–S bond strength of the pyS ligand when coordinated to the $[\text{Ru}(\text{CN})_5]^{3-}$ moiety. Comparatively to the data obtained for the desorption process of the pyS monolayer, the reductive desorption potentials, E_{rd} , present shifts of -170 and -110 mV for the Ru and Fe complexes, respectively. The voltammetric curves of cytochrome c (cyt c) performed with the MpySAu electrodes showed electrochemical parameters consistent with that reported for the native protein. These results taken together reinforce that the π back-bonding effect from the $[\text{M}(\text{CN})_5]^{3-}$ metal center [Ru (4d) $>$ Fe (3d)] strongly affects the MpySAu adlayer stability, reflecting the adlayer performance on the assessment of the cyt c hET reaction.

Introduction

The functionality of a variety of inorganic monolayers formed by molecules of moderate sizes, which are characterized by strong intramolecular charge transfer (CT), has been claimed in the fabrication of film wave guides, sensors, transducers, detectors, electronic displays and as optical materials. To efficiently prepare films for a specific application, one must assemble appropriate molecular functionalities on the metal substrates.¹ Actually, many applications require amphifunctional adsorbed molecules, *i.e.* molecules with one part that has strong affinity for metallic surfaces and another that has either weak or no affinity. In the case of thiolate molecules, it is well documented² that the strong specific interaction between the sulfur atom and the gold surface induces the spontaneous assembly of an adsorbed monolayer at the gold–solution interface. This spontaneous interface process of modifying surfaces, offers the possibility of forming ordered and highly packed monolayers.^{2,3} Additionally, the use of an amphifunctional adsorbate for a specific application requires a particular chemical characteristic of the terminal functional group.

The electrochemical study of metalloproteins such as cytochrome c (cyt c) with conventional metal electrodes is not straightforward. Many structural aspects of cyt c leave the metal ion site “buried” up to 10 Å into the protein, making its exposure to the electrolyte medium difficult.⁴ According to the literature,^{5,6} the molecular recognition of gold electrodes chemically modified by organic molecules toward the cyt c heterogeneous electron transfer (hET) reaction is strongly dependent on the adlayer geometrical arrangement and the

chemical characteristics of the functional terminal group. It seems that, in addition to an optimum chemical interaction between the modifier terminal functional group and the cyt c lysine ends, an extremely organized and highly packed monolayer is required.

For 4-mercaptopyridine (pyS) derivatized modifiers on gold electrodes (pySAu), *in situ* SERS (surface enhanced Raman scattering) experiments have demonstrated that the electron density on the sulfur atom is strongly affected by the electron donor properties of the pyS *p*-substituent.⁷ Recently, it has been reported⁸ that both pySAu adlayer stability and its efficiency on the assessment of the cyt c hET reaction are enhanced upon coordination to the $[\text{Ru}(\text{CN})_5]^{3-}$ moiety (RupySAu). Accounting for the fact that the organic surfaces are typically less ordered and less stable than their inorganic counterparts,⁹ the stability enhancement of RupySAu in relation to the pySAu electrode was assigned to the $p_{\pi}(\text{pyS}) \leftarrow d_{\pi}(\text{Ru}^{\text{II}})$ π -back-bonding electron density capability of Ru^{II} . This effect increases the RupyC–S bond strength making more difficult the oxidative cleavage process that has been attributed as the main reason for the structural destruction of the pyS monolayer on gold electrodes.¹⁰

Aiming to gain a better understanding on the effectiveness of the electronic properties of the $[\text{M}(\text{CN})_5]^{3-}$ metal centers on the pyS monolayer stability, we prepared the $[\text{Fe}(\text{CN})_5(\text{pyS})]^{4-}$ (FepyS) complex as a new gold modifier applicable for the assessment of the cyt c hET reaction. Its well known that the π -back-bonding effect is strongly dependent on the radial extension of the nd_{π} orbitals involved.¹¹ As the cyanide environment and the negative electronic charge are the same in

Table 1 Retention time (min), half-wave formal potentials (mV) and electronic spectra data (nm)

Compound	Retention time ^a	$E_{1/2}$ ^b	λ_{\max} ^c	f^d
[Ru(CN) ₅ (pyS)] ⁴⁻	2.5	780	390, 322, 288	0.342
[Fe(CN) ₅ (pyS)] ⁴⁻	3.0	220	405, 320, 229	0.176
pyS	5.0	–	322, 290	–

^a Analytical $\lambda = 254$ nm. ^b Vs. Ag/AgCl, 25 °C, $\mu = 0.10$ M (NaCF₃-COO), pH = 4.0. ^c Aqueous solutions. ^d Oscillator strength.

both Ru and Fe complexes, the difference in the π -electron-donating character of these metals elects them as good probe molecules to evaluate the role of $p_{\pi^*}(\text{pyS}) \leftarrow d_{\pi}(\text{M}^{\text{II}})$ π -back-bonding on monolayer stability and as a facilitator toward the cyt c hET reaction.

Results and discussion

The characterization of the FepyS complex was carried out by high performance liquid chromatography (HPLC); cyclic voltammetry; electronic, infrared, and Raman spectroscopies.

The retention time acquired from the HPLC chromatograms, summarized in Table 1, indicates, under the experimental conditions employed, that the RupyS complex is more hydrophilic than the FepyS and pyS species. It is well accepted that the cyt c residues surface require a hydrophilic environment for best molecular recognition. Given this factor, and considering that the positive-charged lysine groups close to the cyt c surface are hydrophilic residues, it is reasonable to anticipate that the RupyS modifier on gold would be better interacting to assess the hET reaction of this protein relative to FepyS and pyS promoters.

The half-wave formal potential, $E_{1/2} = 220$ mV, for the Fe^{III/II} redox process indicates a thermodynamic stability of the Fe^{II} toward its oxidized Fe^{III} state, and a reduced metal center stability gain compared to the starting material [Fe(CN)₅(NH₃)]³⁻ (electrochemical data, $E_{1/2} = 135$ mV). The cyanometalate M^{II} redox stabilization compared to its oxidized M^{III} counterpart is currently assigned to $p_{\pi^*}(\text{CN}^-) \leftarrow (nd_{\pi})^6(\text{M}^{\text{II}})$ interactions.¹¹ In the case of the [Ru(CN)₅(pyS)]^{3-/4-} redox process, $E_{1/2} = 780$ mV, the significantly more positive potential value is explained by the larger radial extension of the 4d _{π} orbitals that facilitates the $p_{\pi^*}(\text{CN}^-) \leftarrow (nd_{\pi})^6(\text{M}^{\text{II}})$ interactions, compared to the 3d _{π} orbitals of the analogous iron species.

The electronic spectrum of the [Fe(CN)₅(pyS)]⁴⁻ ion complex in aqueous solution shows intense absorption bands at 405 nm ($\epsilon = 3.42 \times 10^2 \text{ M}^{-1} \text{ cm}^{-1}$) and 230 nm ($\epsilon = 2.44 \times 10^3 \text{ M}^{-1} \text{ cm}^{-1}$) assigned to metal to ligand charge transfer (MLCT), $p_{\pi^*}(\text{pyS}) \leftarrow d_{\pi}(\text{Fe}^{\text{II}})$ and $p_{\pi^*}(\text{CN}^-) \leftarrow d_{\pi}(\text{Fe}^{\text{II}})$ transitions, respectively.¹² An additional shoulder observed at 320 nm was assigned to the pyS $\pi^* \leftarrow \pi$ intraligand transition.¹³ Although the energy of the MLCT band of the FepyS complex is energetically favored relative to that for RupyS species, an increase of about 50% is observed in the oscillator strength for the Ru^{II} complex (Table 1). This oscillator strength ratio is in good agreement with that calculated for similar Ru^{II} and Fe^{II} systems,¹⁴ and suggests a stronger $p_{\pi^*}(\text{pyS}) \leftarrow (nd_{\pi})^6(\text{M}^{\text{II}})$ π -back-bonding intensity in the ruthenium complex.¹⁵

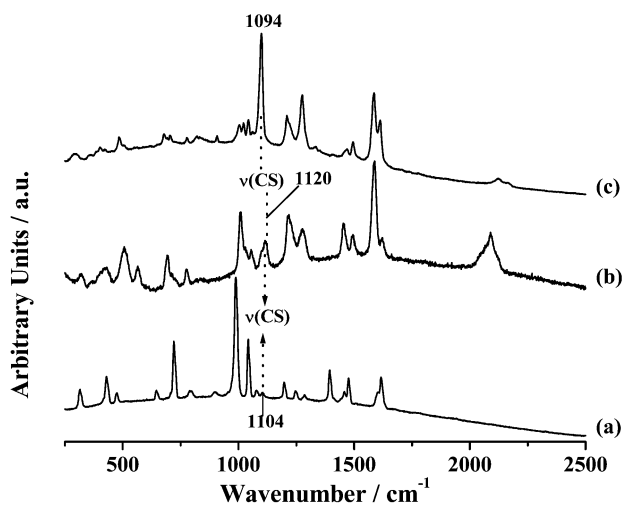
The Raman vibrational spectrum for the FepyS complex in the solid state, along with that of the uncoordinated pyS ligand are shown in Fig. 1. The frequency values are given in Table 2.

The FepyS spectrum (Fig. 1(b)) is similar to that obtained for RupyS complex, and presents the typical bands at 1120 and 2042 cm⁻¹ assigned to the $\nu(\text{C}=\text{S})$ and $\nu(\text{CN}^-)$ stretching modes of the pyS thiolate and cyanide groups, respectively.^{16,18} Since the frequency of the $\nu(\text{C}=\text{S})$ mode is strongly affected by the nature of the *trans* substituent on the pyridine ring,^{7,19} the shift observed on this frequency mode (currently attributed in the literature^{17,19,20} as an X-sensitive band) from 1104 cm⁻¹ in

Table 2 Vibrational spectra assignments for Na₄[Fe(CN)₅(pyS)]·4H₂O in the solid state and adsorbed onto a gold polycrystalline surface

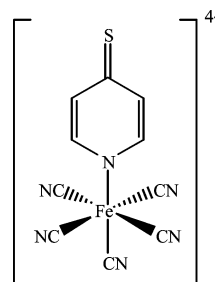
Assignment ¹⁶⁻²⁰	Wavenumber/cm ⁻¹	
	Normal Raman	SERS
$\delta(\text{C-S})/\gamma(\text{CCC})$	425 (m)	375 (w)
$\gamma(\text{CCC})$	507 (m)	490 (w)
$\nu(\text{Fe-CN})$	576 (w)	–
$\beta(\text{CCC})$	694 (m)	683 (w), 709 (w)
$\beta(\text{CC})/\nu(\text{C-S})$	721 (sh)	–
$\gamma(\text{CH})$	776 (w)	781 (w)
Ring breathing	1011 (vs), 1060 (m)	998 (w)
Ring breathing/ $\nu(\text{C-S})$	1120 (m)	1096 (vs)
$\beta(\text{CH})$	1220 (s), 1280 (m)	1208 (m), 1280 (s)
$\nu(\text{C}=\text{C}=\text{N})$	1455 (s), 1495 (m)	1470 (w), 1498 (m)
$\nu(\text{CC})$	1587 (vs), 1622 (w)	1587 (s), 1616 (s)
$\nu(\text{C}\equiv\text{N})$	2089 (s)	2121 (w)

sh = shoulder, w = weak, m = medium, s = strong, vs = very strong.

**Fig. 1** Normal Raman spectra of (a) pyS and (b) Na₄[Fe(CN)₅(pyS)]·4H₂O in the solid state and (c) SERS spectrum of the gold electrode modified after 5 min immersion in a 20 mM aqueous solution of the [Fe(CN)₅(pyS)]⁴⁻ ion complex.

the spectrum of the pyS ligand (Fig. 1(a)) to 1120 cm⁻¹ in the FepyS spectrum (Fig. 1(b)) suggests nitrogen coordination to the iron metal center. Another evidence is the shift to higher wavenumber (1640 cm⁻¹) of the C=C pyridine ring stretching,¹⁷ compared with the pyS free ligand spectrum at 1617 cm⁻¹. Also, the $\nu(\text{CN}^-)$ frequency value indicates that the iron metal center ion is in the Fe^{II} reduced oxidation state. A shift of about 70 cm⁻¹ to higher frequency is expected for the analogous Fe^{III} complex.²¹ Therefore, upon coordination to the Fe^{II} metal center, the sulfur atom of the pyridine thiolate ligand is available for chemisorption interactions with metallic surfaces.

Based on the arrangement shown in Chart 1, the following adsorption site possibilities can be proposed: (i) sulfur atom; (ii) π orbitals of pyridine ring and (iii) nitrogen atom of the cyanide groups.

**Chart 1** Structure representation of the [Fe(CN)₅(pyS)]⁴⁻ ion complex.

The SERS spectrum of the gold electrode modified after 5 min of immersion in 20 mM aqueous solution of the FepyS complex (Fig. 1(c)) however, indicates the pyS sulfur atom as the most probable adsorption site. The spectrum presents pyridine group vibrational modes more intense than of the cyanide group stretching frequencies. This observation suggests, according to surface selection rules,²² that the pyS moiety is closer to the gold surface than the CN⁻ groups. The FepyS SERS spectrum (Fig. 1(c)) is dominated by the intense signals of the in-plane vibrational modes of the pyS ($\beta(\text{CH})$ and $\nu(\text{C}=\text{C}/\text{C}=\text{N})$ from 1200 to 1616 cm⁻¹), indicating a perpendicular orientation on the gold substrate.^{6,19} The shift in the $\nu(\text{CS})$ band from 1120 cm⁻¹ in the solid state vibrational spectrum (Fig. 1(b)) to 1094 cm⁻¹ in the adlayer spectrum (Fig. 1(c)), indicates a lowering in the double bond character of the C–S bond. This observation, together with that of the increase of intensity of the $\nu(\text{C}=\text{S})$ intensity band (Fig. 1(c)), suggest that the complex adsorption process towards the gold substrate occurs through the sulfur atom *via* a σ interaction. This effect is attributed to the coupling between the 12a₁ ring breathing and the $\nu(\text{C}=\text{S})$ stretching modes.^{23–25} Similar results were observed^{8,19,20} in the SERS spectra of RupyS and pyS species adsorbed on gold surfaces.

Electrochemical desorption data

The reductive desorption curves, illustrated in Fig. 2, were acquired by linear sweep voltage (LSV) in the potential range from –0.2 to –1.2 V. The gold electrodes were modified by using different immersion times in 20 mM aqueous solutions of the FepyS, pyS and RupyS promoters.

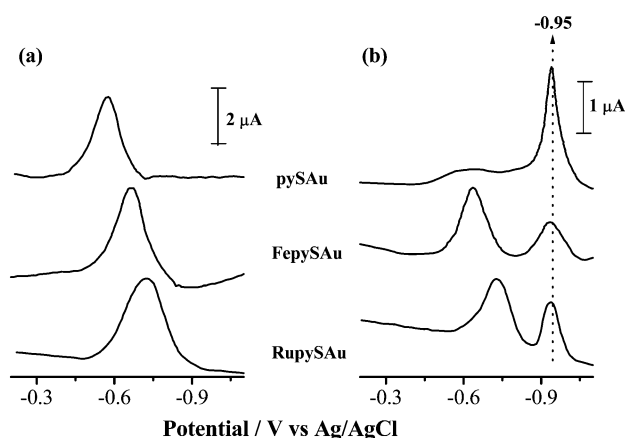
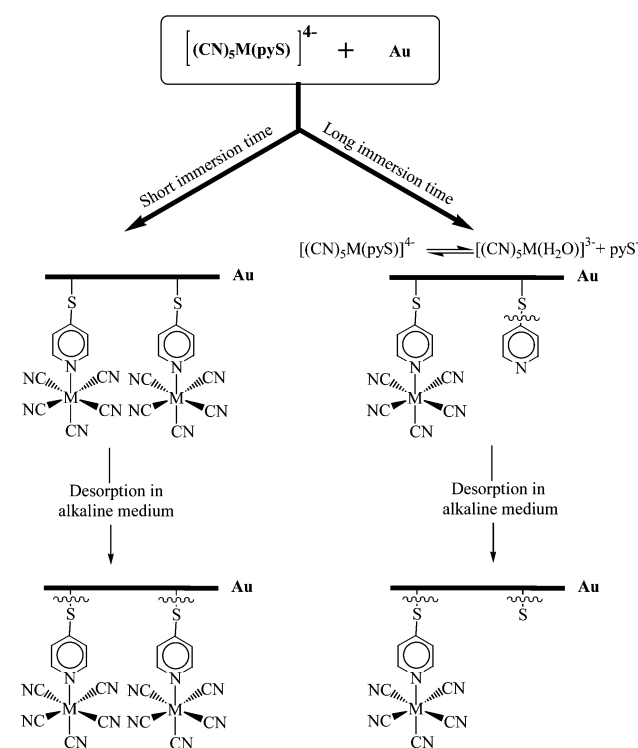


Fig. 2 Linear sweep voltammetry (LSV) desorption curves of pyS, FepyS and RupyS monolayers formed onto gold at 100 mV s⁻¹ in 0.5 M KOH solution after (a) 5 and (b) 30 min immersion in solutions of the respective promoters.

The desorption curves obtained after 5 min of immersion (Fig. 2(a)) present the waves assigned^{26,27} to Au–SR, R = py, Rupy or Fepy. The more negative reductive desorption potential, $E_{\text{rd}} = -0.73$ V, indicates that the RupyS monolayer is more strongly bound to surface than the FepyS ($E_{\text{rd}} = -0.67$ V) and pyS ($E_{\text{rd}} = -0.56$ V) species. These results are in good agreement with the π -back-bonding effect assignment,⁸ which enhances the electronic density of the pyS pyridine ring, improving the chemisorption process of the ruthenium and iron cyanometalates. The $E_{\text{rd}}(\text{RupyS}) < E_{\text{rd}}(\text{FepyS})$ potential order can be explained based on the nd_{π} orbital radial extension. The more stabilized Ru^{II} 4d _{π} orbitals interact strongly with the energetically appropriated pyS π^* orbitals compared with that of Fe^{II} 3d _{π} orbitals.¹⁴ As consequence, an enhancement of the electronic density of the pyS thiolate moiety makes the RupyS adsorbate thermodynamically more stable toward the desorption process than the FepyS species on gold surfaces. These results hint that the stability of the pySR adlayer on gold is strongly related to the electronic density on thiolate sulfur.⁷

As the immersion time is increased, a new wave at –0.95 V is observed in all Au–SR adlayer desorption curves (Fig. 2(b)). This wave has been assigned to a reductive desorption electrode reaction of a monolayer composed of undesirable sulfur forms.¹⁰ The reductive desorption curves for FepySAu surface compared to that reported for RupyS adsorbed on gold,⁸ show that the –0.95 V wave starts to appear over a smaller time scale (*ca.* 15 and 30 min of immersion in 20 mM FepyS and RupyS aqueous solution, respectively).

Accounting for the $[(\text{CN})_5\text{M}(\text{pyS})]^{4-}$ aquation reaction, the pseudo-first-order rate constant for the iron species, $k_{\text{obs}} = 1.1 \times 10^{-3}$ s⁻¹, is one order of magnitude faster than that observed for the ruthenium complex.¹² This result indicates that the free pyS ligand is earlier present in solution, in the time scale of the FepyS electrode modification procedure, and the wave at –0.95 V could derive from pySAu adlayer decomposition instead of FepySAu degradation. According to the aquation rate, $t_{1/2} = 10$ min, the competitive adsorption of the dissociated free pyS ligand must be considered for smaller immersion times relative to the RupySAu adlayer.⁸ Scheme 1 illustrates the MpySAu structural conversion leading to a monolayer formed by atomic and/or oligomeric sulfur forms.



Scheme 1 Diagram of $[(\text{CN})_5\text{M}(\text{pyS})]$ -Au adlayer degradation by desorption processes in alkaline medium as a function of immersion time.

The competitive adsorption process assignment is strengthened by the SERS spectrum of the gold substrate obtained for longer immersion times (up to 24 h) in a 20 mM aqueous solution of the FepyS complex. Similarly to the RupySAu adlayer SERS spectra,⁸ and in an opposite behavior to the reflectance FTIR and SERS spectra recorded for pyS monolayers formed at gold after longer immersion times,^{8,28} the spectrum of the FepySAu presented neither band intensity decrease nor frequency shifts in relation to those obtained after 5 min immersion time (Fig. 2(c)). However, conclusions cannot be made about the concurrent pyS adsorption based on the SERS spectra acquired after longer immersion times in the FepyS or RupyS aqueous solution because of surface selection rules.²² The SERS technique presents a signal intensification of the species closest to the surface. In this way, the signals due to

Table 3 cyt c hET k^0 (cm s^{-1}) values obtained for different electrodes^{a,b}

Electrode	$10^3 k^0$
AuRupyS	7.91 ^c
AuFepyS	6.80
AupyS	6.00 ^d

^a Nicholson's method. ^b 0.1 mM KH_2PO_4 (pH = 7). ^c Ref. 8. ^d Ref. 31.

the pyS molecules adsorbed in consequence of the aquation process would be hidden by the FepyS and RupyS bands.

Electroactivity of FepySAu electrodes toward the cyt c electrochemistry

The efficiency of the FepySAu electrode in the assessment of the cyt c hET reaction was analyzed by cyclic voltammetry, and compared with that obtained with the RupySAu electrode (Fig. 3).

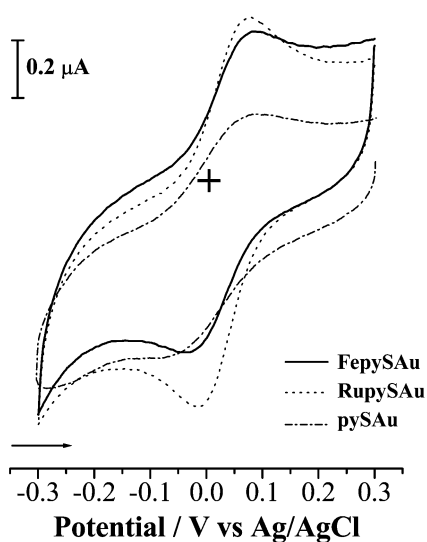


Fig. 3 Cyclic voltammograms at 50 mV s^{-1} of 1 mM cyt c in 100 mM KH_2PO_4 , pH = 7, solution with FepySAu, RupySAu and pySAu electrodes.

Both RupySAu and FepySAu surfaces were obtained after 5 min immersion in 20 mM aqueous solutions of the respective promoters. The cyclic voltammograms present a redox process with a typical half-wave potential of 20 mV for the heme- $\text{Fe}^{\text{III/II}}$ heterogeneous process of native cyt c protein.²⁹ The difference between the anodic and cathodic potential peaks, ΔE_p , and the cathodic current peaks, $-i_{\text{pc}}$, values indicate that the RupyS modified electrode presents the best performance to assess the rapid cyt c hET process, as described by the heterogeneous electron transfer rate constant values, k^0 , described in Table 3.

Based on the chromatographic data, this result is in accordance with the greater hydrophilic character of the RupyS complex (Table 1). The lysine residues close to the protein surface are hydrophilic and positively charged at physiological pH, thus requiring a hydrophilic surface for a better interaction. As the electrode immersion time increases, deformation in the shape of the voltammetric curves was observed (Fig. 4) with a decrease in the i_{pc} values and an increase in ΔE_p , suggesting a slower electron transfer kinetics. In fact, the typical cyt c Faradaic process is absent in the curve obtained at 50 mV s^{-1} after 120 min of immersion (Fig. 4(d)).

The cyt c voltammetric curve deterioration observed after longer immersion times indicates a decrease in the ability of the promoter FepyS to facilitate the hET reaction of this metalloprotein. A similar behavior was observed by Lamp *et al.*¹⁰ by using pyS as gold electrode modifier. The authors suggest that

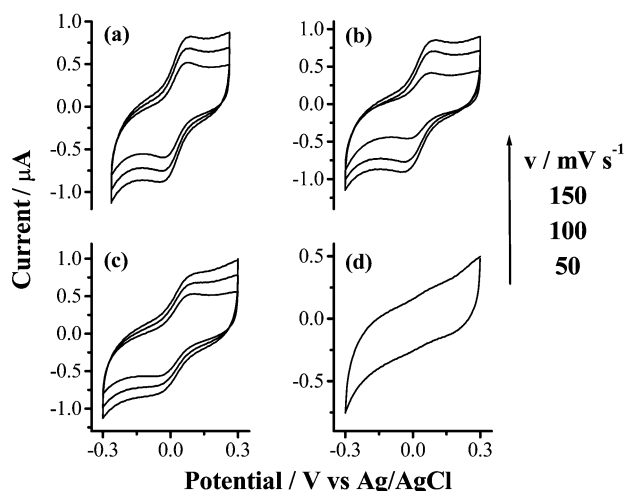


Fig. 4 Cyclic voltammograms at 50, 100 and 150 mV s^{-1} of cyt c at gold electrodes immersed for (a) 5, (b) 15, (c) 30 and (d) 120 min in 20 mM FepyS aqueous solution. Electrolysis conditions: 1 mM cyt c in 100 mM KH_2PO_4 , pH = 7.

a structural conversion of the pyS monolayer occurs on the surface, resulting in an adlayer composed by atomic and/or oligomeric sulfur forms.¹⁰ Although the LSV data have indicated that an identical effect occurs for the monolayer formed by FepyS onto gold, the SERS spectrum did not show clear evidence for this. Even after 24 h of immersion time preparation of gold electrode, the SERS spectrum remained essentially unchanged. This behavior can be attributed to the pyS monolayer stability gain upon coordination of pentacyanoiron(II). Although the k^0 value for the cyt c redox protein with the FepySAu electrode is of the same order of magnitude (Table 3), it is slightly higher than those reported in the literature for the pyS, pySSpy promoters,³¹ and lower than for the RupyS¹² monolayer.

Conclusions

The $[(\text{CN})_5\text{M}(\text{pyS})]^{4-}$, M = Fe and Ru, complexes form stable monolayers on roughened gold electrode surfaces. The pyS ligand is coordinated to both metal centers through the pyridine ring nitrogen atom. Upon coordination to Ru^{II} and Fe^{II} metal centers, the sulfur atom of the pyridine thiolate ligand remains available to adsorb on the gold surface.

The SERS data for the monolayers formed by iron and ruthenium complexes on gold clearly show the increase in the intensity of the vibrational modes of the pyridine ring moiety compared to the cyanide stretching frequencies. Therefore, on the basis of surface selection rules, one can conclude that the pyS coordinated ligand is closer to the electrode than the cyanides. The $\nu(\text{C}=\text{S})$ band observed at 1120 cm^{-1} in both RupyS and FepyS normal Raman spectra shifted to 1096 and 1094 cm^{-1} in the adlayers SERS spectra, respectively, thus indicating a decrease of the double bond character of the C–S bond. Also, the $\nu(\text{C}=\text{S})$ band intensity increase observed in the SERS spectra suggests a perpendicular arrangement of the adsorbates in relation to the surface normal.

Assuming the potentials for the reductive desorption processes are dependent on the strength of the Au–S interaction, the reductive LSV data for RupyS ($E_{\text{rd}} = -0.73$ V), FepyS ($E_{\text{rd}} = -0.67$ V) and pyS ($E_{\text{rd}} = -0.56$ V) monolayers freshly prepared on gold allow the conclusion that the complexes are more strongly bound to gold than the pyS free ligand.

The results also indicate that a more stable monolayer is formed by the RupyS complex compared to FepyS. This is consistent with the $p_{\pi^*}(\text{pyS}) \leftarrow d_{\pi}(\text{M}^{\text{II}})$ π -back-bonding capability of the metal center ion¹¹ [Ru^{II} (4d) > Fe^{II} (3d)] constituent of the monolayer, that affects the electronic density on

the sulfur atom of the head group portion of the modifier molecule, improving the chemisorption process. The ability for metal–ligand orbital interactions is enhanced if the metal d orbitals extend far into space, enabling effective overlap with π^* ligand orbitals.

The wave at -0.95 V, typical of adlayer degradation, appears on both reductive LSV curves for the complexes monolayers prepared by longer immersion times. This wave starts to appear for the FepySAu desorption in a smaller time scale than that for the RupyS adsorbate, allowing the conclusion that RupyS is more strongly bound to gold than FepyS.

The fact that the cyt c electrochemical response decreases with an increase in the immersion time modification in the FepyS solution reinforces the conclusion previously made from the reductive desorption experiments. The irregularity of the monolayer in consequence of the concurrent pyS adsorption (Scheme 1) seems to be responsible for the FepyS adsorbate performance decrease in the assessment of the cyt c hET reaction, compared with the RupyS adsorbate.

The results all together suggest that the structural stability of a pyS monolayer is strongly affected by the electronic properties of the $[\text{M}(\text{CN})_5]^{3-}$ substituent on the pyridine ring, exhibiting a good correlation with the chemical properties of the ruthenium and iron cyanometalate complexes.

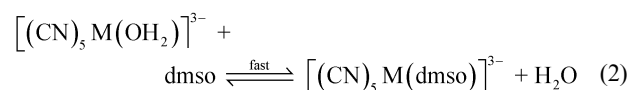
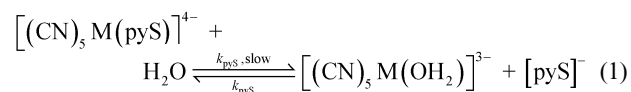
Experimental

The water used throughout was purified by a Milli-Q system (Millipore Co.). $\text{Na}_3[\text{Fe}(\text{CN})_5(\text{NH}_3)] \cdot 4\text{H}_2\text{O}$ was synthesized according to the literature.¹² The organothiol ligand, 4-mercaptopyridine (pyS), KOH, and KH_2PO_4 , from Aldrich, were used without previous purification. The Suprapur H_2SO_4 from Merck was used as received. Horse heart cytochrome c (type VI, 99%, Aldrich Co.) was purified as described in the literature.³² The $\text{K}_4[\text{Ru}(\text{CN})_5(\text{pyS})] \cdot 3\text{H}_2\text{O}$ (RupyS) complex was synthesized according to the literature procedure.^{8,14}

The $\text{Na}_4[\text{Fe}(\text{CN})_5(\text{pyS})] \cdot 4\text{H}_2\text{O}$ (FepyS) complex was prepared according to the literature procedures¹⁴ for similar complexes preparations, with minor modifications. A 50 mg sample of $\text{Na}_3[\text{Fe}(\text{CN})_5(\text{NH}_3)] \cdot 4\text{H}_2\text{O}$ was dissolved in 2 mL of water followed by the slow addition of a 5-fold excess (~ 80 mg) of the 4-mercaptopyridine ligand dissolved in 6 mL of water. The resulting solution developed an intense brown color and was allowed to stand for 1 h in the absence of light, under stirring, and argon flow. The reaction mixture was then cooled in an ice-bath and added dropwise to a cooled saturated NaI ethanolic solution, under vigorous stirring. A red–brown precipitate was formed and collected by filtration, washed with ethanol and diethyl ether, dried, and stored under vacuum in the absence of light. Anal. Calc.: C: 26.09; H: 2.63; N: 18.27. Found: C: 26.31; H: 2.59; N: 18.58%.

Kinetic measurements

The aquation reaction of $[\text{Fe}(\text{CN})_5(\text{pyS})]^{4-}$ (eqns. (1) and (2)) was studied in the presence of a large excess of dimethyl sulfide (dmsO) as auxiliary ligand, at 25 ± 0.2 °C:



An aliquot of the $[\text{Fe}(\text{CN})_5(\text{pyS})]^{4-}$ complex solution was added to a solution containing dmsO, both previously deaerated, at 25 °C. The disappearance of the $[\text{Fe}(\text{CN})_5(\text{pyS})]^{4-}$

metal-to-ligand charge transfer (MLCT) band was monitored spectrophotometrically at $\lambda_{\text{max}} = 405$ nm. In order to avoid contributions of the back-reaction, k_{pyS} , the concentration of the $[\text{Fe}(\text{CN})_5(\text{pyS})]^{4-}$ complex was kept lower than 1.0×10^{-4} M. Specific rate constants were calculated from the plots of $\log(A_\infty - A_t)$ vs. time. These plots were linear for more than three half-lives.

Apparatus

The electronic spectra of aqueous solution of the complexes and ligand were acquired with a Hitachi model U-2000 spectrophotometer.

The chromatographic analyses were performed with a Shimadzu liquid chromatograph equipped with a model LC-10AD pump and an SPD-M10A UV-Visible photodiode-array detector with a CBM-10AD interface. An ODS column (250 mm \times 4.6 mm id., 5 μm particles; from Altech) was used with an isocratic elution with 10 : 90 acetonitrile–water containing 0.1% HTFA, pH = 3.7. The chromatograms were taken at a constant flow-rate of 1.0 mL min^{-1} . Samples for analyses were dissolved in the mobile phase and the 5 μL volumes were injected.

The transmission infrared spectra of the compounds dispersed in KBr were obtained by using a Perkin-Elmer instrument model Spectrum 1000.

Electrochemical experiments were performed with an electrochemical analyzer BAS 100W from Bioanalytical System at 25 ± 0.2 °C. A conventional three-electrode glass cell with a glassy carbon (~ 0.13 cm² geometrical area) and a platinum foil were used as working and auxiliary electrodes, respectively, for the complex characterization.

The electrochemical experiments with cyt c were carried out by using a three-electrode configuration cell, using 0.1 M buffer phosphate (KH_2PO_4), pH = 7.0 as electrolyte, at 25 ± 0.2 °C. Before the experiments, the cyt c solutions were stored at 4 °C in order to avoid protein denaturation.⁴ Gold surface modified with the promoters and a gold flag, were used as working and auxiliary electrodes, respectively. The cyclic voltammetry simulation curves for scan rates higher than the limit diffusion control, required for the heterogeneous electron transfer rate constant calculation, were obtained by using DIGISim 2.1 BAS software.

For acquisition of the reductive desorption curves, a Teflon cell was used to prevent KOH electrolyte chemical attack on the glass apparatus. A 0.03 cm² polycrystalline gold surface and a gold flag were used as working and auxiliary electrodes, respectively.

The *ex situ* SERS spectra of the monolayers formed by the pyS ligand and FepyS complex were acquired by using a Renishaw Raman Imaging Microscope System 3000 equipped with a CCD (Charge Coupled Device) detector, and an Olympus (BTH2) with 50 \times objective to focus the laser beam on the sample in a backscattering configuration. As exciting radiation, λ_0 , the 632.8 nm line from a He–Ne (Spectra-Physics) laser, was used. The gold substrates used for spectra SERS acquisition were activated by the ORC procedure in 0.1 M KCl as described by Gao *et al.*,³³ without the active species in solution with minor modifications. The activation of the gold surface for SERS spectra acquisition was made by using a PAR 273 potentiostat. The activated substrates were acquired after 25 oxidation–reduction cycles (ORC) at 100 mV s^{-1} from -0.3 to $+1.2$ V, holding at $+1.2$ V for 1.2 s.

The polishing procedure of the gold surfaces employed in the different experiments above cited, was made as described by Qu *et al.*³⁴ These electrodes were mechanically polished with alumina paste of different grade to a mirror finish, rinsed and sonicated (10 min) with Milli-Q water. Then, the electrode was immersed in a freshly prepared “piranha solution” (3 : 1 concentrated H_2SO_4 –30% H_2O_2) (CAUTION: “piranha

solution” is a strong oxidant solution that reacts violently with organic compounds), rinsed exhaustively with water and sonicated again. The cleanness was evaluated by comparison of the *i* vs. *E* curve obtained in a 0.5 M H₂SO₄ solution with the well established curve for a clean gold surface.³⁵

All experimental procedures were performed at room temperature and the potentials cited throughout are quoted relative to an Ag/AgCl/3.5 M KCl electrode.

The surface modification procedure was made by immersing the gold electrodes in a 20 mM aqueous solution of the FePyS complex. For comparative purposes, gold surface modifications with pyS ligand and RupyS complex were also performed by similar procedures.

Acknowledgements

The authors are thankful to the Brazilian agencies CNPq, CAPES and FAPESP, for financial support. I. S. M., I. C. N. D. and J. R. de S. gratefully acknowledge CNPq and FAPESP for the grants of the fellowships (301220/94-8/CNPq, 300560/00-1/CNPq, and 99/02438-4/FAPESP, respectively).

References

- 1 L. H. Dubois and R. G. Nuzzo, *Annu. Rev. Phys. Chem.*, 1992, **43**, 437.
- 2 H. Sellers, A. Ulman, Y. Shnidman and J. Eilers, *J. Am. Chem. Soc.*, 1993, **115**, 9389.
- 3 M. D. Porter, T. B. Bright, D. L. Allara and C. F. D. Chidsey, *J. Am. Chem. Soc.*, 1987, **109**, 3559.
- 4 F. A. Armstrong, *Struct. Bonding (Berlin)*, 1990, **72**, 137.
- 5 I. Taniguchi, *Redox Chem. Interfacial Behav. Biol. Mol.*, 1988, 113.
- 6 T. Sawaguchi, F. Mizutani and I. Taniguchi, *Langmuir*, 1998, **14**, 3565.
- 7 C. A. Szafranski, W. Tanner, P. E. Laibinis and R. L. Garrel, *Langmuir*, 1998, **14**, 3580.
- 8 I. C. N. Diógenes, F. C. Nart, M. L. A. Temperini and I. S. Moreira, *Inorg. Chem.*, 2001, **40**, 4884.
- 9 L. Strong and G. M. Whitesides, *Langmuir*, 1988, **4**, 546.
- 10 B. D. Lamp, D. Hobara, M. D. Porter, K. Niki and T. M. Cotton, *Langmuir*, 1997, **13**, 736.
- 11 H. Taube, in *Electron Transfer Reactions*, ed. S. S. Isied, Advanced Chemical Series, Washington, 1997, vol. 253, pp. 1–17.
- 12 P. Ford, D. F. P. Rudd, R. Gaunder and H. Taube, *J. Am. Chem. Soc.*, 1968, **90**, 1187.
- 13 A. Albert and G. B. Barlin, *J. Chem. Soc.*, 1959, 2384.
- 14 I. S. Moreira and D. W. Franco, *Inorg. Chem.*, 1994, **33**, 1607.
- 15 C. R. Johnson and R. E. Shepherd, *Inorg. Chem.*, 1983, **22**, 2439.
- 16 K. Nakamoto, *Infrared and Raman Spectra of Inorganic and Coordination Compounds*, Wiley, New York, 3rd edn., 1978.
- 17 J. H. S. Green, W. Kynaston and H. M. Paisley, *Spectrochim. Acta*, 1963, **19**, 549.
- 18 E. Spinner, *J. Chem. Soc.*, 1963, 3860.
- 19 J. Baldwin, N. Schuler, I. S. Butler and M. P. Andrews, *Langmuir*, 1996, **12**, 6389.
- 20 H.-Z. Yu, N. Xia and Z.-F. Liu, *Anal. Chem.*, 1999, **71**, 1354.
- 21 L. Tosi, *Spectrochim. Acta, Part A*, 1973, **26**, 353.
- 22 J. A. Creighton, Selection Rules for Surface-Enhanced Raman Spectroscopy, in *Spectroscopy of Surfaces*, ed. R. J. H. Clark and R. E. Hester, John Wiley & Sons, Chichester, UK, 1988.
- 23 M. A. Bryant, S. L. Joa and J. E. Pemberton, *Langmuir*, 1992, **8**, 753.
- 24 T. H. Joo, M. S. Kim and K. J. Kim, *Raman Spectrosc.*, 1987, **18**, 57.
- 25 K. Carron and L. G. Hurley, *J. Phys. Chem.*, 1991, **95**, 9979.
- 26 D. E. Weissar, M. M. Walczak and M. D. Porter, *Langmuir*, 1993, **9**, 323.
- 27 C.-J. Zhong and M. D. Porter, *J. Am. Chem. Soc.*, 1994, **116**, 11616.
- 28 I. C. N. Diógenes, F. C. Nart, M. L. A. Temperini and I. S. Moreira, *Electroanalysis*, 2002, **14**, 153.
- 29 M. J. Eddowes and H. A. O. Hill, *J. Am. Chem. Soc.*, 1979, **101**, 4461.
- 30 R. S. Nicholson, *Anal. Chem.*, 1965, **37**, 1351.
- 31 I. Taniguchi, K. Toyosawa, H. Yamaguchi and K. Yasukouchi, *J. Electroanal. Chem.*, 1982, **140**, 187.
- 32 D. L. Brautigan, M. S. Fergusson and E. Margoliash, *Methods Enzymol.*, 1978, **53**, 128.
- 33 P. Gao, D. Gosztola, L.-W. H. Leung and M. J. Weaver, *J. Electroanal. Chem.*, 1987, **233**, 211.
- 34 X. Qu, T. Lu and S. Dong, *J. Mol. Catal.*, 1995, **102**, 111.
- 35 D. T. Sawyer, A. Sobkowiak and J. L. Roberts Jr., *Electrochemistry for Chemists*, John Wiley & Sons, New York, 2nd edn., 1995.